REPORT DOCUMENTATION PAGE

Form Approved
OMB NO. 0704-0188

1. AGENCY USE ONLY *(Leave blank)*	2. REPORT DATE	3. REPORT TYPE AND DATES COVERED
		REPRINT

4. TITLE AND SUBTITLE

TITLE ON REPRINT

5. FUNDING NUMBERS

DAAL03-92-G-0122

6. AUTHOR(S)

AUTHOR(S) ON REPRINT

7. PERFORMING ORGANIZATION NAMES(S) AND ADDRESS(ES)

UNIVERSITY OF WISCONSIN - MADISON
MADISON, WI 53706

8. PERFORMING ORGANIZATION REPORT NUMBER

9. SPONSORING / MONITORING AGENCY NAME(S) AND ADDRESS(ES)

U.S. Army Research Office
P.O. Box 12211
Research Triangle Park,, NC 27709-2211

10. SPONSORING / MONITORING AGENCY REPORT NUMBER

ARO 30340.77-EG-URI

11. SUPPLEMENTARY NOTES

The views, opinions and/or findings contained in this report are those of the author(s) and should not be construed as an official Department of the Army position, policy or decision, unless so designated by other documentation.

12a. DISTRIBUTION / AVAILABILITY STATEMENT

Approved for public release; distribution unlimited.

12 b. DISTRIBUTION CODE

13. ABSTRACT *(Maximum 200 words)*

ABSTRACT ON REPRINT

DTIC QUALITY INSPECTED 4

14. SUBJECT TERMS			15. NUMBER IF PAGES
			16. PRICE CODE

17. SECURITY CLASSIFICATION OR REPORT	18. SECURITY CLASSIFICATION OF THIS PAGE	19. SECURITY CLASSIFICATION OF ABSTRACT	20. LIMITATION OF ABSTRACT
UNCLASSIFIED	UNCLASSIFIED	UNCLASSIFIED	UL

Injection Pressure Effects Upon Droplet Behavior in Transient Diesel Sprays

Calvin C. Hung and Jay K. Martin
University of Wisconsin-Madison

Ja-Ye Koo
Hankuk Aviation Univ.

GLOBAL MOBILITY *DATABASE*

All SAE papers, standards, and selected books are abstracted and indexed in the SAE Global Mobility Database.

Injection Pressure Effects Upon Droplet Behavior in Transient Diesel Sprays

Calvin C. Hung and Jay K. Martin
University of Wisconsin-Madison

Ja-Ye Koo
Hankuk Aviation Univ.

ABSTRACT

This paper reports on the investigation of injection pressure upon the droplet behavior in transient diesel sprays. Phase/Doppler results for a Diesel spray with a maximum fuel injection line pressure of 105 MPa are compared with previously acquired droplet size and velocity measurements for a Diesel spray with an injection pressure of 21 MPa. All measurements reported here were made in atmospheric conditions at a position near the nozzle.

It is shown in these results that the droplet velocity and size profiles do maintain similarity despite the substantial change in injection pressure. Specific characteristics, for example, the appearance of subtle waves in the time-dependent spray data, are present in both data sets.

Comparison of the measured droplet velocities and diameters with Weber number based stability criteria shows that increased injection pressure produces a higher percentage of droplets that are likely to breakup. This is mostly the result of increases in droplet velocities with higher injection pressure.

The interior region of the higher pressure spray is an area extremely difficult to probe, despite the application of temporal optimization of the phase/Doppler anemometer. Inherent characteristics of the injection that affect the ability to acquire data are described, as well as some of the operational difficulties experienced in using a phase/Doppler for diesel spray droplet measurements.

INTRODUCTION

In the past several years, there have been a number of Diesel fuel spray studies examining droplet sizes and velocities. The work performed has provided some insight towards a basic understanding of Diesel sprays and sprays in general [1-6]*. In the quest for improved emissions, however, fuel distribution strategies have changed. Certain techniques have been shown to be effective in reducing certain emissions. Probably the most well known tactic is increased injection pressure [7]. Work has been done with high pressure fuel injection systems [7-11], but part of what remains to be discovered is a comprehensive understanding of the effect of increased injection pressure on droplet behavior.

The intent of this work is to examine the microscopic characteristics of a high pressure (105 MPa) Diesel fuel spray and determine how increased injection pressure affects the spray droplet behavior. This is accomplished by comparing the experiment data with data acquired previously on a low injection pressure (21 MPa) Diesel spray system [12-14] (which will henceforth be referred to as the low pressure system). In both cases, data was provided by a He-Ne based Phase Doppler Particle Analyzer at atmospheric conditions.

EXPERIMENT SET UP & PROCEDURE

INJECTION SYSTEMS & INSTRUMENTATION- In comparing data from two difference experiments, it is important to take note of the experiment set up for both experiments and their instrumentation. Figure 1 is a general schematic of the experiment set up for both Diesel fuel injection systems. For both injection systems, the arrangement consisted of a single hole injector pointing downward into a glass enclosure which was open to atmosphere. This atmospheric spray chamber is composed of four 38.1 cm x 30.5 cm glass plates held in an aluminum frame. There is an exhaust pipe and drip tank at the bottom. The mass flow rate of air due to the ventilation into the exhaust pipe was kept low enough to not adversely affect the Diesel spray behavior.

---

* Numbers in brackets designate references enumerated in the Reference List.

The low pressure system consisted of a Bosch PE4P100 injection pump turned by a DC motor at 800 rpm. The fuel injection pump was modified for one cylinder use. Pump shaft rotational position was monitored with a 12-bit absolute optical encoder that furnished crankangle data to the phase/Doppler system with a resolution of 0.1°. The injector was a Lucas-CAV injector with a type J nozzle (No. 4518930) and a static popping pressure of 15.2 MPa. The nozzle hole diameter and length were 0.24 mm and 0.8 mm, respectively. Also, the injector was equipped with a Hall effect sensor to measure needle lift and strain gauges to measure injection pressure. The fuel injection line was physically constrained to a length of approximately 1.5 m.
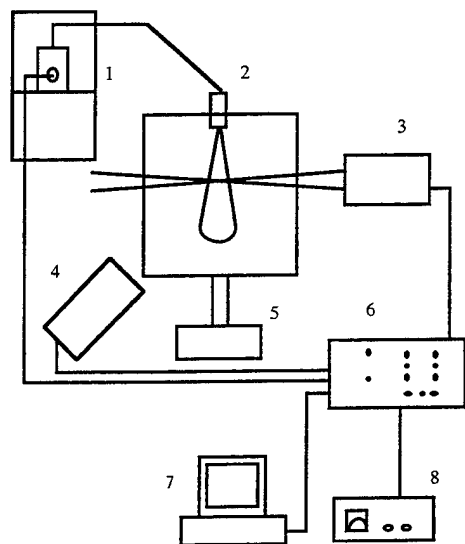
1.Fuel pumping system with optical encoder
2.Injector mounted atop the atmospheric spray enclosure
3.Phase/Doppler transmitter
4.Phase/Doppler receiver
5.Fuel exhaust/drip tank
6.Phase/Doppler signal processor
7.Computer
8.Oscilloscope

Figure 1. Schematic of Experiment

The fuel used for the low pressure injection system was Phillips No. 2D Diesel fuel, which had a density of 848 kg/m³, a kinematic viscosity of 2.5 x 10⁻⁶ m²/s and a refractive index of 1.4748. Approximately 9.0 mg of fuel was sprayed per injection.

The high pressure injection system utilized a dedicated pump test stand turning a Nippondenso EP-9 fuel injection pump at 800 rpm. Crankangle data regarding the EP-9 was provided by the same 12-bit absolute optical encoder used with the low pressure system. The single hole injector was a Nippondenso injector with the same nozzle hole dimensions as in the low pressure injection system. However, the needle opening pressure was set at a higher pressure, 28.6 MPa. The injector itself was not instrumented for fuel pressure, but fuel injection line pressure was measured

monitored with a pressure transducer (PCB 118A02). The pressure transducer was mounted roughly 12 cm from the injector. The injector was outfitted with a Hall effect sensor to measure needle lift like the injector for the low injection pressure system. The injection line length was minimized to approximately 0.9 m. Longer fuel line lengths tended to add undesirable variability to the injections.

The high pressure injection system was run with Amoco Premier Diesel fuel. This fuel has a density of 857.1 kg/m³, a kinematic viscosity of 2.54 x 10⁻⁶ m²/s and a refractive index of 1.48. Fuel injection quantity was measured to be 13.4 mg per injection.

For comparison, the two systems were matched in fuel injection parameters such as pump speed, nozzle hole length, and nozzle hole diameter. In addition, fuel properties were similar. The main difference between the two systems is the injection pressure. The high pressure system has a peak injection pressure of 105 MPa while the injection pressure of the other system crests at one fifth of that level, 21 MPa. Other differences between the two systems, such as fuel injection quantity and injection line length, exist due to the intent of injecting fuel at a desired pressure and proper operation of the system.

Droplet information was gathered from both systems by a 1-D Phase Doppler Particle Analyzer with a 10 mW He-Ne laser. In both cases, the phase/Doppler system was set up with the receiver 30° off-axis and oriented to measure velocities in the vertical plane with positive velocities being in the downward direction. The phase/Doppler anemometer was set on a traversing table to allow measurements of various locations.

The phase/Doppler system used in acquiring data from the low pressure injection system was a counter-based system employing a rotating diffraction grating in the transmitter for beam splitting and frequency shifting. The optical set up provided a size range of 7.1 to 250 μm for the first track of the rotating diffraction grating. The second track allowed a size range of 2.3 to 80.6 μm, and the third track had a size range of 2.0 to 70.0 μm. The optimal track choice was dependent upon measurement location within the spray.

For the high pressure system, the phase/Doppler system was upgraded to a Fourier transform-based system. A Bragg cell is employed in the transmitter instead of rotating diffraction grating. With a 500 mm transmitter lens, the system had an available size range of 4.7 - 250.0 μm. This appeared to be the most appropriate transmitter lens for the spray in terms of droplet diameter range and resolution out of the available lens choices. While this admittedly and unfortunately neglects an expected number of droplets less than 4.7 μm in diameter, there was little indication during the experiment of any significant number of droplets greater than 250 μm.

MEASUREMENT LOCATIONS - Phase/Doppler measurements were taken of the high pressure Diesel

spray in several locations. These locations are noted in Table 1, where z is the distance in centimeters along the spray axis from the nozzle tip and r is the perpendicular distance in millimeters from the spray axis. The relative position of these locations to the spray boundary is seen in Figure 2. From spray schematic in Figure 2, one can see that the spray is fairly narrow in atmospheric conditions, leaving radial measurement locations limited to within several millimeters at most.

z (cm) \ r (mm)	-5	0	3	5	9
1		•			
2		•			
3		•	•		
4		•	•		
5		•			
6	•	•		•	•

Table 1. Schematic of the phase/Doppler measurement locations. (Note: Schematic not to scale.)
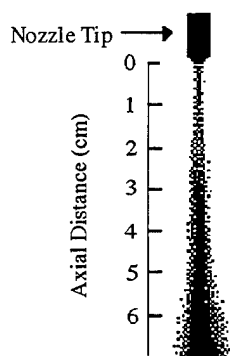

Nozzle Tip →

Figure 2. Scaled Schematic of Spray

Measurement locations were made with consideration of planned future measurements of the Diesel spray under elevated temperature and pressure conditions as well as space limitations. Furthermore, several of the measurement locations are consistent with the measurements taken for the Diesel spray with a low injection pressure. These measurement locations also include one point for a simple spray symmetry check.

TEST METHODOLOGY - It has been well established that the examination of the microscopic characteristics of a dense Diesel spray is difficult, especially within the inner core of the spray near the nozzle. Phase/Doppler measurements do not prove to be the exception.

Difficulties with making measurements in a dense Diesel spray with a phase/Doppler anemometer stem from the limitations of the phase/Doppler system in dealing with the inherent characteristics of a high pressure Diesel spray. Problematic characteristics of a high pressure Diesel spray include high droplet number density, non-spherical droplets, an extensive droplet size and velocity range, and the transient nature of the spray. The high droplet number density causes degradation of

the laser beams before the probe volume, degradation of the refracted light after the probe volume, mixing of the signal with light noise scattered from particles outside the probe volume, and invalidation of signals due to the single particle constraint of the phase/Doppler anemometer. The phase/Doppler is also constrained by the necessity of droplet sphericity in the probe volume for valid measurement and a dynamic size range that has a maximum droplet size to minimum droplet size ratio of 35.

While it will take extensive work to address the above mentioned problems, the one problematic characteristic of a Diesel spray that can be dealt with somewhat easily is the transient nature of the spray. The transient nature of the spray difficulty refers to the fact that the nature of the spray changes over time. This creates a problem when making phase/Doppler measurements as the instrument settings can not be set to vary with time. The varying nature of the spray also makes it rather difficult to optimize the performance of the phase/Doppler.

One solution is to divide up the spray into sections temporally. This is possible with crankangle input to the phase/Doppler system from the absolute optical encoder mounted on the fuel injection pump. By windowing the data to a certain crankangle range, the phase/Doppler can be set for optimal measurement of droplet sizes and velocities within that window.
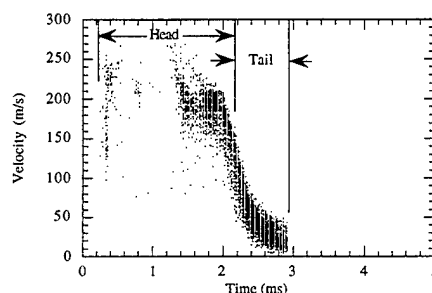

Figure 3. Indication of temporal measurement division on the velocity profile for the high pressure Diesel spray at z = 4 cm, r = 0 mm.

For on-axis measurements of the high pressure Diesel spray, the spray was temporally divided into two sections, which are referred to here as the head and the tail. The dividing line was set at approximately the transition point where the droplet velocities began to decrease. An example of this is shown in Figure 3. For each section, 5,000 valid measurements were taken with the phase/Doppler system. Off-axis measurements did not necessarily require temporal division of the spray as the variation of droplet sizes and velocities is not as great in these regions. The off-axis measurements still maintained the sample number of 10,000 valid droplet measurements. This is also consistent with the sample number taken in the 21 MPa injection pressure spray experiment.

3

The challenge of taking data within the core of a Diesel spray also comes from optimization of the phase/Doppler system. In particular, the voltage setting for the photomultiplier (PMT) detectors becomes significant. A low voltage setting will detect the strong Doppler signals of large droplets, but will not be able to distinguish the weak Doppler signals of small droplets from the high noise encountered. Increasing the PMT voltage enables the phase/Doppler anemometer to detect small droplets, but it also causes an increase in noise and possible oversaturation of the large droplet signals. This is troublesome mostly along the axis of the spray where the range of droplet sizes and the extent of noise are the greatest.
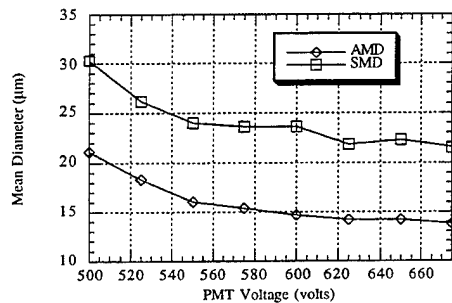

Figure 4. Variation of AMD and SMD with PMT voltage for spray location z = 6 cm and r = 5 mm.

The value of the PMT voltage plays a large part in determining the distribution of droplets measured. Consequently, computed values such as the Arithmetic Mean Diameter (AMD) and the Sauter Mean Diameter (SMD) are affected by the PMT voltage setting. This is shown in Figure 4 for data taken at z = 6 cm and r = 5 mm for the entire spray. The data points are the averages for runs with 1000 samples. From the figure, it is clear that the PMT voltage does vary the AMD and SMD values. Increasing the PMT voltage from 500 volts to 675 volts decreases the SMD by approximately 26% and the AMD value by 33%. Such variation becomes more significant for on-axis measurements where the range of droplet sizes is broadest.

It should be noted though that the trend of AMD and SMD with respect to PMT voltage is highly dependent upon the available droplet diameter distribution. If the available droplet distribution is a wide distribution, then improved ability to measure the smaller droplets with increasing PMT voltage may cause the SMD to increase due to increasing influence of the large droplets upon the SMD calculation. A narrow droplet distribution would have the opposite effect because the influence upon the SMD calculation of a small droplet in the distribution is close to that of a large droplet.

To attempt to reduce the effect that PMT voltage has upon the data, a specific methodology for taking phase/Doppler measurements was adopted. This allows the data to at least be consistent in how they were acquired.

Along the spray axis, a number of data runs with varying PMT voltage settings were made before the actual experiment measurements were conducted. The PMT voltage was ultimately set for the experiment at the point where the AMD stopped declining. This was done for each individual location and for the head and tail sections of the spray.

As mentioned before, increasing the PMT voltage would allow the detection of smaller droplets, thus decreasing the AMD. Eventually, the voltage increases should reach a point where the number of small droplets able to be detected is maximized. Consequently, there is a risk of oversaturation of the large droplet signals at this point which might cause a bias toward small droplets, but other Phase Doppler Particle Analyzer parameters, such as maximum diameter and maximum velocity, were fixed to accommodate as many large droplets as reasonably possible since large droplets have a very significant effect on SMD values.

Unfortunately, this method has the drawback of being very conducive to picking up noise, so it was no surprise that the validation percentages was consistently low, with many of the rejections being attributed to failure of meeting the minimum signal to noise ratio criteria. Along the axis, the number of valid measurements only amounted to 4 to 7 percent of the attempted measurements for the head of the spray. The tail of the spray experienced slightly better validation percentages, with values ranging from 10 to 15 percent.

Off-axis measurements were easier as the ranges of droplet diameters and velocities were smaller. As a result, the spray event was not divided up temporally. The PMT voltage was set using the same method applied for on-axis measurements. Phase/Doppler measurements for the low injection pressure spray did not employ temporal division either. The PMT voltage was also set at the point of minimal change in the AMD.

The last significant issue with operation of the Phase Doppler Particle Analyzer involves choice of appropriate limits in the intensity validation scheme. As a further check against erroneous measurements, the phase/Doppler system utilizes user chosen limits for acceptable droplet signal intensity. Theoretically, the signal intensity of a measured droplet is directly proportional to its diameter. System realities, however, sometimes produce small droplets with high signal intensity and large droplets with small signal intensity. Typically, these erroneous measurements are fairly distinct and can be eliminated by setting the intensity validation limits to accept only those measurements having a reasonable relationship between size and scattering intensity.

However, in using the phase/Doppler system to make measurements within a Diesel spray, setting these limits becomes somewhat difficult. In Figure 5, an example plot of intensity versus diesel spray droplet diameter data is shown with the example upper and lower intensity limits shown as the solid black curves.

4

The theoretical trend would follow a curve from the lower lefthand corner to the upper righthand corner. However, there are no obvious clues to how the intensity validation limits should be set, leaving the possibility of some variation in the data acquisition. A specific methodology for setting this limits has not been established yet. This problem of where to set the intensity validation limits is currently being examined.
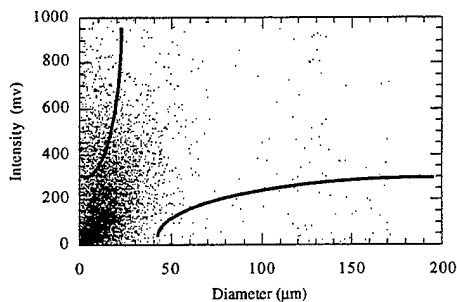

Figure 5. *Example plot of intensity versus diameter measurement for near nozzle diesel spray measurements.*

INJECTION SYSTEM CHARACTERISTICS - Although the 105 MPa injection system and the 21 MPa injection system are similar in many characteristics, no two fuel injection systems are exactly alike. The way a fuel injection system behaves can be determined from plots of such items as rate of injection and fuel injection pressure.
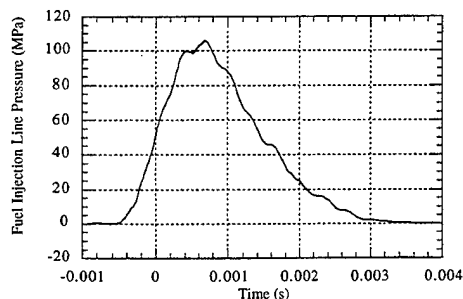

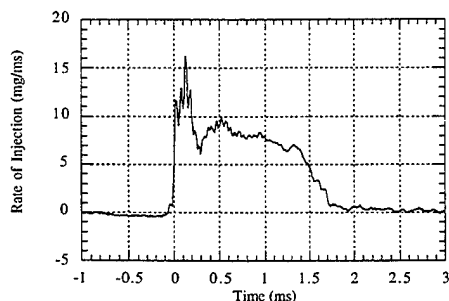*Figure 6.* *Fuel injection line pressure trace of the high pressure fuel injection system.*

Figure 7 *Rate of injection of the high pressure fuel injection system.*

Figure 6 shows the fuel line injection pressure trace for the high pressure injection system. The rate of injection for the same system is displayed in Figure 7. It is important to note though that the injection rate trace in Figure 7 is believed to be affected to some extent by noise. In particular, the high spike in the beginning of the injection is most likely due to noise, and that the actual maximum height probably does not exceed 14 mg/ms.

Figure 8 and Figure 9 display has the same type of plots for the low pressure system. In comparing these scanned plots [12] with those of the low pressure system, the respective curves appear show somewhat similar in shape, but there are enough differences to indicate one of the limitations of this study.
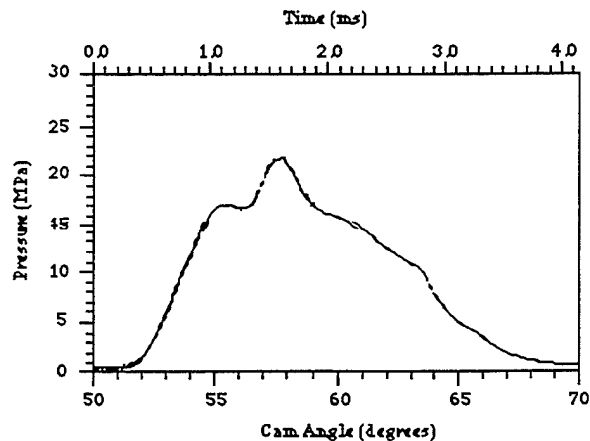

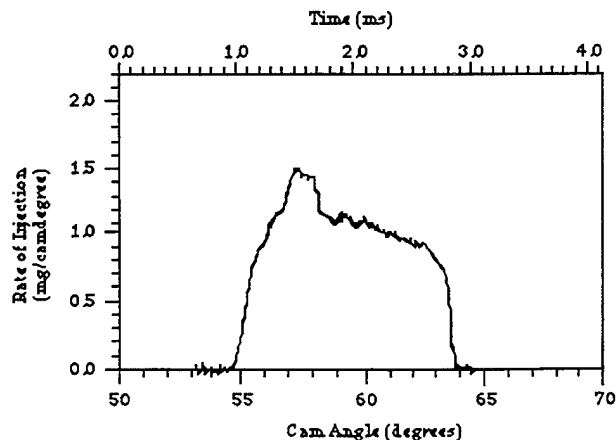*Figure 8.* *Fuel injection pressure curve of the low pressure system. Plot scanned from [12].*

Figure 9. *Rate of injection of the low pressure fuel injection system. Plot scanned from [12].*

In this experiment, it was assumed that the spray was axisymmetric. To validate this assumption, a check was made by taking data on opposite sides of the spray for comparison. Shown in Figure 10 is the diameter histogram for the point z = 6 cm and r = 5 mm. Figure 11, the diameter histogram for the location z = 6

cm and r = -5 mm, is very comparable to Figure 10. Other measured and computed items, such as run time, mean velocity, AMD, SMD, and validation percentage, were also consistent.
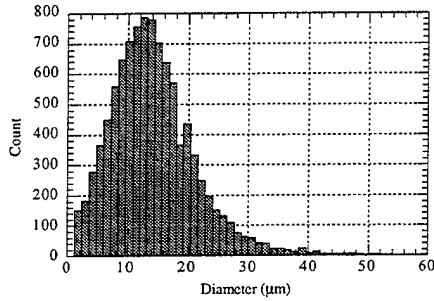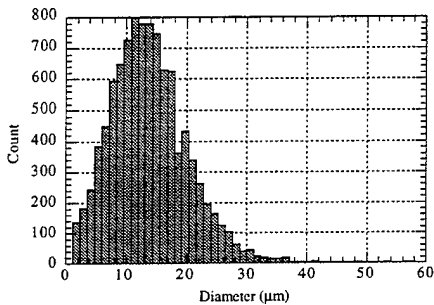

Figure 10.   Diameter Histogram for z = 6 cm, r = 5 mm.

Figure 11.   Diameter Histogram for z = 6 cm, r = -5 mm.

DISCUSSION OF RESULTS

For the 105 MPa Diesel spray, on-axis phase/Doppler results did not present a complete profile of the spray until the measurement volume was moved 3 cm from the nozzle tip. Droplet measurements for the head of the spray were not possible at distances of 1 cm and 2 cm along the axis.

Phase/Doppler results for the on-axis position of z = 3 cm are shown in Figure 12. These profiles of droplet diameter and velocity reveal that the main body of spray, the head, is traveling at approximately 200 m/s on average and is composed of droplets with diameters ranging from at least 7.14 μm to 250 μm, the entire phase/Doppler size range. Although the data gives the appearance that the majority of droplets are less than 100 μm in diameter for the head of the spray, there is a significant number of droplets around 200 μm in diameter which cannot be ignored. This broad spectrum of droplet sizes is one example of the challenge faced when attempting to take measurements with a phase/Doppler anemometer.

The velocity profile reveals that most of the droplet velocities in the head of the spray fall between 160 m/s and 225 m/s. The indication from this narrow band of droplet velocities in the velocity profile plot is

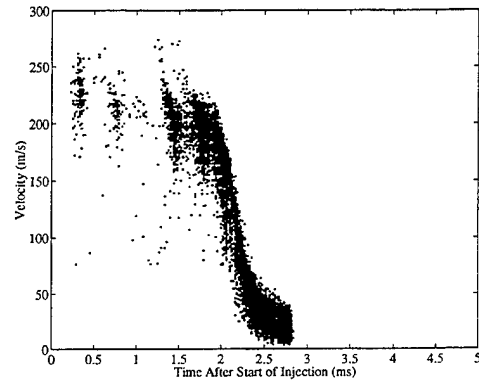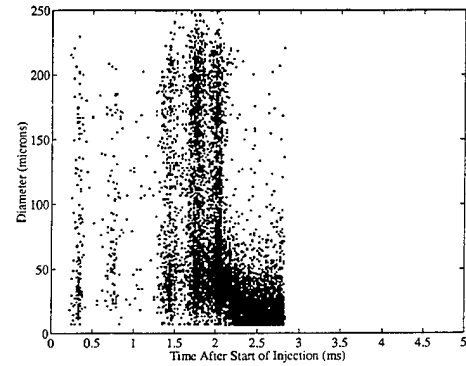that drop size has little or no correlation with size in the head of the spray.

Figure 12.   Phase/Doppler data for the on-axis location z = 3 cm of the 105 MPa injection pressure Diesel spray.
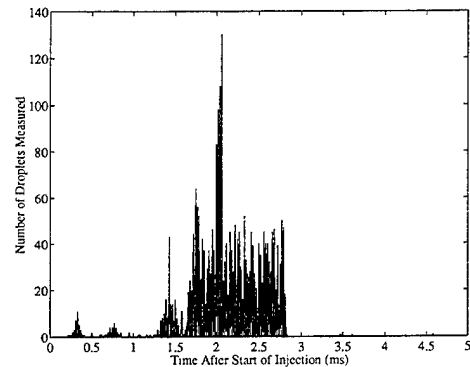

Figure 13.   Number of droplets measured as a function of time for on-axis location z = 3 cm of the 105 MPa diesel injection spray.

The visible gaps of data within the head of the spray suggest that the spray possesses a wave-like distribution of droplets. This is better seen in Figure 13, which gives the number of droplets measured for each 0.02083 ms, or 0.1° crankangle. This plot shows that validated data rate is higher at certain portions of the spray and practically non-existent in others. As there is no variation in phase/Doppler operational parameters for the head and tail sections of the spray, the only item affecting data acquisition is the spray itself. The possible explanations for the data gaps are thus limited to either that these gaps are areas of high droplet

6

number density, regions where droplet non-sphericity is prevalent, or both. The largest data gap lies between 0.8 ms and 1.3 ms after the start of injection, the middle of the head of the spray.

Velocity only measurements for the high pressure diesel spray at 3 cm from the nozzle along the spray axis are shown in Figure 14. This figure shows a very similar profile to the velocity profile obtained with diameter measurement capability on. The appearance of the same data gaps, albeit not as distinct as the diameter case, indicates that droplet non-sphericity is only a limited factor for the lack of data at certain times within the head of the spray.
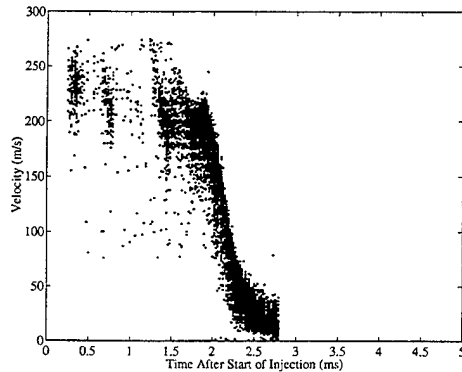

Figure 14. *Velocity profile for the 105 MPa injection pressure spray at z = 3 cm and r = 0 mm. Data taken with the phase/Doppler anemometer set up for velocity only measurements.*
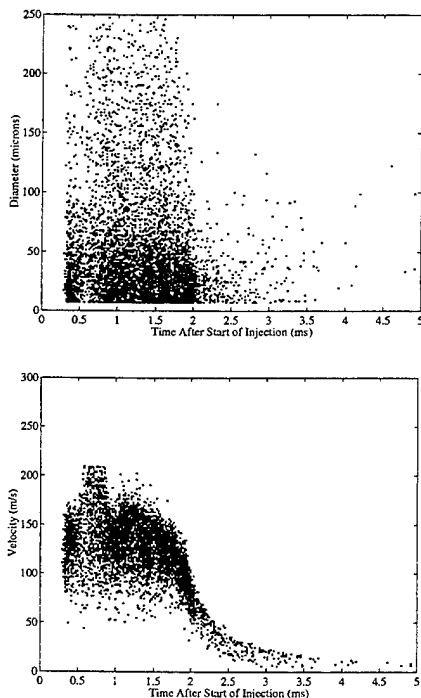

Figure 15. *Phase/Doppler data for the on-axis location z = 3 cm of the 21 MPa injection pressure Diesel spray.*

Figure 15 shows the phase/Doppler data for the same location in the low injection pressure spray. There are several similarities between the low injection pressure spray data and the high injection pressure spray data. For instance, the general profile is similar for both cases. Droplet velocities and diameters both drop off rapidly at the transition point between the head and the tail. Next, the high injection pressure case has droplet diameters clustering mostly below 75 μm for the head of the spray. The droplet diameters in the low injection pressure data also clusters below 75 μm while the overall distribution stretches the entire measurement range of 7.14 μm to 250 μm.

In both sets of data, the wave-like behavior of the spray is exhibited, albeit more difficult to discern in the low pressure case. Again, the oscillation of droplet data acquisition is better seen in a bar graph displaying the number of droplets measured as a function of time within the injection, as shown in Figure 16.
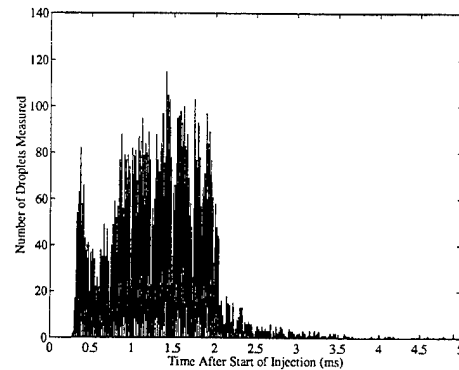

Figure 16. *Number of droplets measured as a function of time for the on-axis location of z = 3 cm of the 21 MPa diesel spray.*

In comparing Figure 12 and Figure 15, a few differences are readily apparent. Droplet velocities only average around 140 m/s for the main body of the spray in the low injection pressure case, but the typical range of drop velocities in the head of the spray is one and a half times that of the high injection pressure case. Drop velocities generally fall between 75 m/s and 180 m/s.

Looking at the diameter profiles, there appears to be a number of droplets larger than 75 μm in the high injection pressure case. In the low injection pressure data, however, drop diameters, although also spread across the entire measurement range, do not look to have the same number of droplets larger than 75 μm. In fact, it appears that the low pressure case has fewer droplets larger than 75 μm than the high pressure case. This is perhaps surprising as a higher injection pressure is thought to produce smaller droplets.

However, there are several issues to consider when assessing this result. The first is that the comparison being made is from phase/Doppler data obtained in two different Diesel sprays, using two different phase/Doppler systems. For example, the lower limit of the intensity validation may not have been

7

stringent enough, allowing some large diameter droplets to be counted despite a low signal intensity. As mentioned before though, setting the limits for intensity validation has not been formalized yet. This leaves the possibility for some variation in the data.

It is also possible that this comparison is a valid indicator of the typical droplet behavior in these sprays. In that case, what is being observed at this measurement location is a difference in droplet sizes because a difference in the temporal evolution of the spray. In other words, at any equivalent axial position, the low pressure spray has had more time for breakup than the high pressure case, and, as will be shown in the data that follows, the drop distribution measured in the high pressure case do evolve to smaller droplets than the low pressure case, consistent with expectations.

The most interesting difference between the high pressure case and the low pressure case is a subtle one. There is a data gap near the head of the spray in Figure 15 approximately 0.55 ms after the start of injection. This data gap has droplet velocities from 80 to 160 m/s in front of it. After the data gap, droplet velocities range from 80 m/s to 210 m/s. The existence of faster droplets after the gap suggests that this position of the injection possesses a number of slower droplets being overtaken and possibly hit by faster droplets from behind.
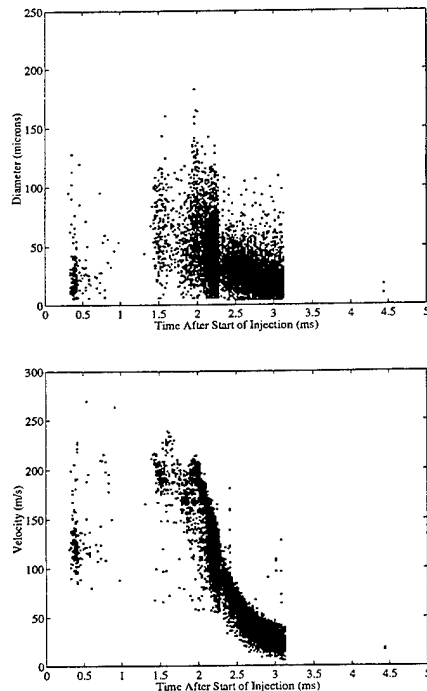
while the measured droplet velocities at the beginning of the spray occur chiefly between 205 m/s and 250 m/s. The apparent conclusion is that near the nozzle the fastest droplets within the spray do not necessarily occur in the middle of the spray for high pressure injection. Hence, one can gather that droplet momentum has not yet been affected by aerodynamic forces to a significant extent.

This changes further downstream, as shown in Figure 17. At this location, the velocities at the tip of the spray lie chiefly around 125 m/s, lower than the quasi-steady portion of the spray behind it, which averages around 190 m/s. In addition, the data gap for the head of the spray has expanded to cover from 0.5 ms after start of injection to 1.5 ms. This data gap expansion to approximately 50% of the head of the spray suggests an increase in droplet number density within the head of the spray.

Droplet diameters have redistributed themselves as well. For the most part, drops larger than 125 μm have faded out of existence. This redistribution of large droplets into smaller drops would mean an increase in number density, assuming not many droplets traveled radially outward. The number density increase would help explain the data gap. In the tail of the spray, droplets settle into a broad band, ranging from 4.7 to 50 μm.
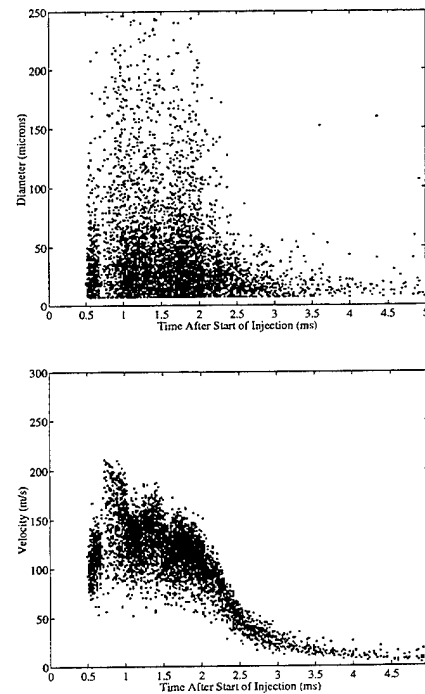

Figure 17. Phase/Doppler data for the on-axis location z = 6 cm. (105 MPa injection pressure case.)

Figure 18. Phase/Doppler data for the 21 MPa injection pressure Diesel spray at on-axis location z = 6 cm.

Looking at the high injection pressure case in Figure 12 (or Figure 14), the gap at the tip of the spray is also present and is centered at 0.6 ms after the start of injection. However, measured droplet velocities at time equals 0.75 ms fall primarily between 200 and 225 m/s

The plots in Figure 17 possess a visible discontinuity within the data. This is a result of the temporal division of the spray into head and tail sections. While somewhat unsightly, this discontinuity does not diminish the validity of the data. It does however present

an excellent example of the limited bandwidth of phase/Doppler instrumentation and how the recorded data is very much a function of the optimization of the instrumentation. For future work, temporal division of the spray into three or more sections would help curb this problem.

Figure 18 shows the data from the low injection pressure spray system for the on-axis location of $z = 6$ cm. In comparing these plots with those of Figure 17, the droplet diameters for the low injection pressure case have not shifted to the lower end to the extent displayed by in Figure 17. In fact, the diameter profile looks remarkably similar to that in Figure 15. The droplet diameters still range from 7.14 μm to 250 μm. There are less droplets greater than 75 μm, especially those greater than 200 μm, and those less than 75 μm are more numerous, but the change is not as significant as in the high pressure case.

In viewing the velocity profile, the low injection pressure case does experience some growth in the data gaps like the high injection pressure case. The wave-like behavior is more apparent in this velocity profile than the one for the on-axis location of $z = 3$ cm. However, the profile still resembles the profile in Figure 15, and the average velocity in the head remains around 140 m/s.
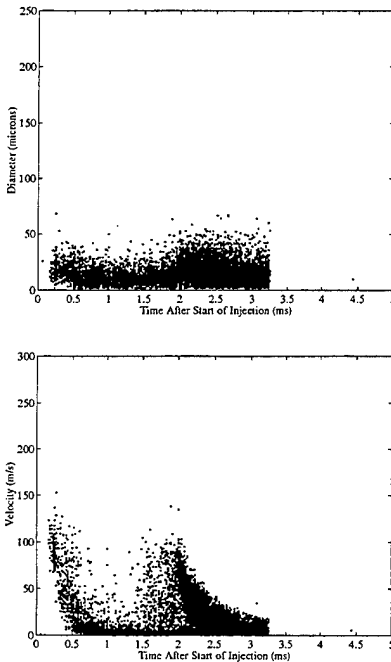

Figure 19. Droplet velocity and diameter profiles for the 105 MPa injection pressure case at $z = 3$ cm, $r = 3$ mm.

At off-axis locations, comparison of droplet diameters proves interesting. Figure 19 and Figure 20 show the velocity and diameter profiles for the high injection pressure case and the low injection pressure case, respectively. The plots exhibit double peaks, although the high injection pressure diameter plot's peaks are heavily subdued. The double peaks correspond to the opening and closing of the injector

needle [12]. The difference between the two profiles is range of droplet sizes and velocity displayed. As one might expect, the high pressure case exhibits droplets spanning a larger range of velocities than the low pressure case. In the diameter plots, the low pressure case has a greater range for the peaks, but the high pressure maintains a wider range overall.

The droplet data acquired can be compared with droplet breakup criteria (or stability criteria) to give an indication of the susceptibility of the droplets to aerodynamic breakup processes. The droplet breakup criteria are a function of non-dimensional parameters, specifically the droplet Weber number and the droplet Reynolds number.
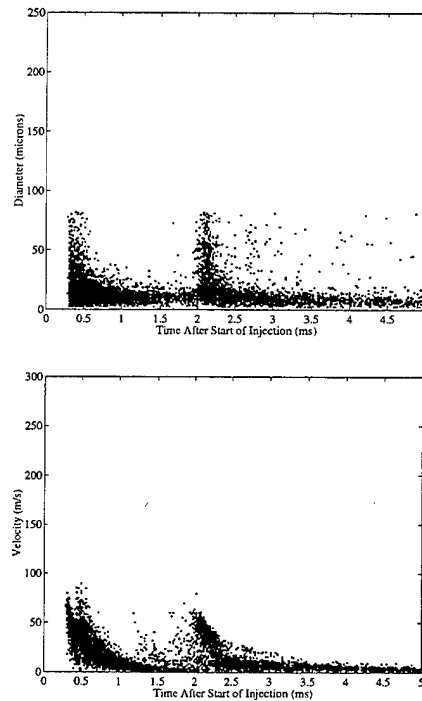

Figure 20. Droplet velocity and diameter profiles for the 21 MPa injection pressure spray at the position $z = 3$ cm, $r = 3$ mm.

Following Reitz and Diwakar [15], the criteria for bag breakup of a droplet is $We_D > 12$. When the criteria

$$\frac{We_D}{Re_D^{1/2}} > 0.5 \qquad \text{(Eq. 1)}$$

is met, the breakup process boundary layer stripping (BLS) is assumed to occur. Droplets not meeting these criteria are assumed to be stable.

In both the droplet Weber number and droplet Reynolds number calculations, the droplet velocity is the relative velocity with respect to the surrounding gas. Since the velocity of the surrounding gas is an unknown, it is impossible to calculate the true droplet Weber number and Reynolds number.

To overcome the lack of knowledge of the true relative velocity of the droplet, two different estimates of

9

relative velocity are made to bound the problem. The first method is to simply use the measured velocity for the relative velocity. This assumes a stagnant gas velocity, making the estimate high in areas where surrounding gas possesses significant velocity from the entrainment process. The second is to assume that the gas velocity is equal to the mean droplet velocity at that point in time and space and take the droplet relative velocity as equal to the absolute value of the droplet velocity minus the average droplet velocity. This method tends to underpredict the relative velocity, but it is more accurate than the first method in areas such as the core of the spray where droplets would have imparted a nonzero velocity to the surrounding gas. The true relative velocity would lie somewhere in between the two estimates.
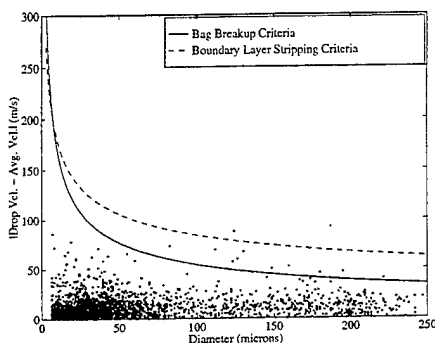
velocities would be too high, but this figure gives some perspective on where the true relative velocity might lie.

Figure 22. *Comparison of 105 MPa injection pressure droplet data at z = 3 cm, r = 0 mm with droplet breakup criteria. The surrounding gas velocity is assumed to be zero.*

Figure 21. *Comparison of 105 MPa injection pressure droplet data at z = 3 cm, r = 0 mm with droplet breakup criteria. The droplet relative velocity is assumed to be the absolute value of the droplet velocity minus the average droplet velocity at that time in the spray.*

Figure 21 is a relative velocity-diameter plot of droplet data for the high pressure case at the on-axis location of z = 3 cm. The plot also includes breakup criteria boundaries for each size class. The bag breakup criteria is represented by squares, and the boundary layer stripping criteria is indicated by triangles.

Figure 21 shows several droplets above the bag breakup criteria. These would be subject to bag breakup, and a few of them, those above the BLS criteria, could also be subject to boundary layer stripping. The droplet relative velocity in this figure is taken as the difference between the droplet velocity and the average droplet velocity for that point in time of the spray. For this location, this method probably gives a better estimate of the true relative velocity. The true relative velocity would likely be somewhat higher, so more droplets than what are shown would exceed the breakup criteria.

In comparison, Figure 22 shows the same data as Figure 21 but with the surrounding gas velocity assumed to be negligible. With this assumption, many of the droplets would be subject to boundary layer stripping. For the core of the spray, these relative
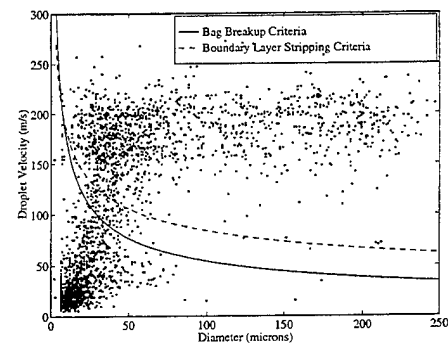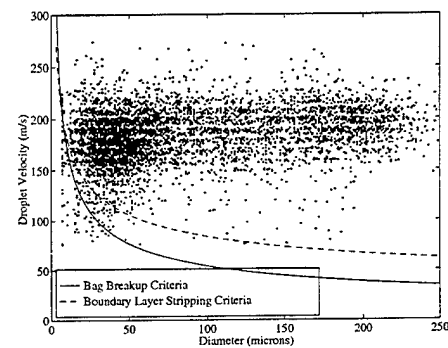

Figure 23. *Comparison of 105 MPa injection pressure droplet data for the head of the spray at z = 3 cm, r = 0 mm with droplet breakup criteria. The surrounding gas velocity is assumed to be zero.*
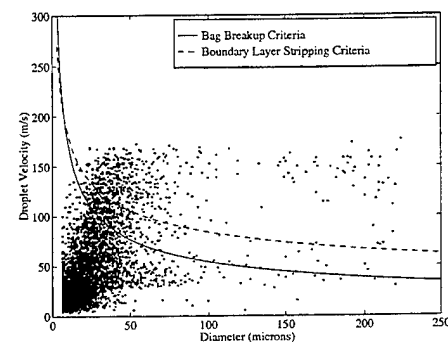

Figure 24. *Comparison of 105 MPa injection pressure droplet data for the tail of the spray at z = 3 cm, r = 0 mm with droplet breakup criteria. The surrounding gas velocity is assumed to be zero.*

Figure 22 contains data for the entire spray. The data can be broken down into the head and tail sections of the spray. Figure 23 contains just the spray head data of Figure 22. Figure 24 shows the data for the tail of the spray.

In Figure 23, the data reveals that almost all of the droplets would undergo boundary layer stripping and bag breakup. Even with a lower droplet velocity closer

10

to the true relative velocity, a majority of droplet within the head would still be subject to breakup processes. The plot also shows quite clearly that the droplets within the head have similar velocities regardless of size.

Figure 24 shows that most of the droplets within the tail of the spray would not be subject to aerodynamic breakup processes. Additionally, the droplets possess a proportional relationship between diameter and velocity not previously seen in the head of the spray.

Figure 25, Figure 26, and Figure 27 show the progression of the spray along the axis at z = 4 cm, 5 cm, and 6 cm, respectively. In these plots, the most noticeable trend is the decline of large droplets with axial distance. While there is a fair number of droplets larger than 150 μm at 4 cm from the nozzle tip, almost all of these droplets disappear by the time the spray reaches z = 6 cm.

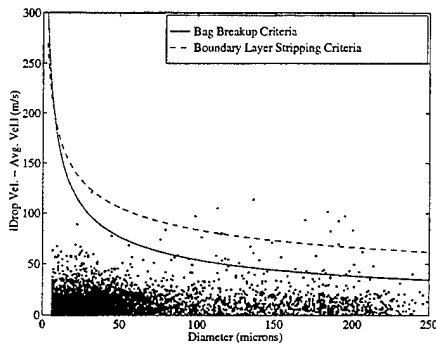*Figure 27. Comparison of 105 MPa injection pressure droplet data at z = 6 cm, r = 0 mm with droplet breakup criteria. The droplet relative velocity is assumed to be the absolute value of the droplet velocity minus the average droplet velocity at that time in the spray.*
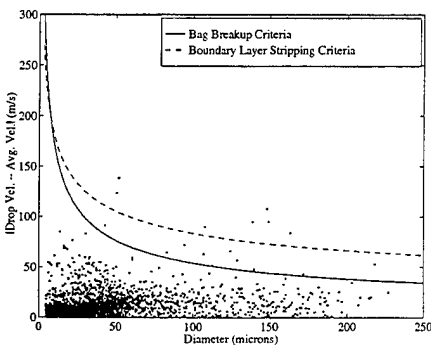

Figure 25. Comparison of 105 MPa injection pressure droplet data at z = 4 cm, r = 0 mm with droplet breakup criteria. The droplet relative velocity is assumed to be the absolute value of the droplet velocity minus the average droplet velocity at that time in the spray.
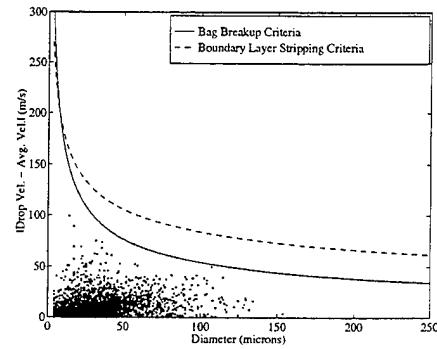
Again, for perspective sake, Figure 28, Figure 29, and Figure 30 show the same data as Figure 25, Figure 26, and Figure 27, respectively, but with the assumption that the surrounding gas velocity is negligible. These plots show the decrease in large droplets with axial distance. They also show that the velocity range is maintained. While the number of slow droplets grows with axial distance, numerous droplets maintain velocities of 200 m/s. This slow decay of droplet velocities is also noted in Figure 25, Figure 26, and Figure 27 where there are consistently several droplets in each graph in excess of the droplet breakup criteria.
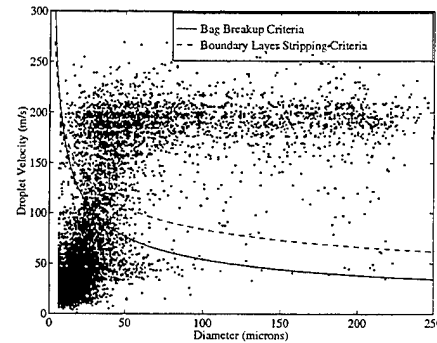

Figure 26. Comparison of 105 MPa injection pressure droplet data at z = 5 cm, r = 0 mm with droplet breakup criteria. The droplet relative velocity is assumed to be the absolute value of the droplet velocity minus the average droplet velocity at that time in the spray.

Figure 28. Comparison of 105 MPa injection pressure droplet data at z = 4 cm, r = 0 mm with droplet breakup criteria. The surrounding gas velocity is assumed to be zero.
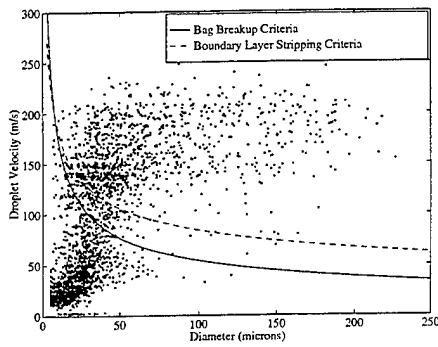
Figure 29. Comparison of 105 MPa injection pressure droplet data
at z = 5 cm, r = 0 mm with droplet breakup criteria.
The surrounding gas velocity is assumed to be zero.
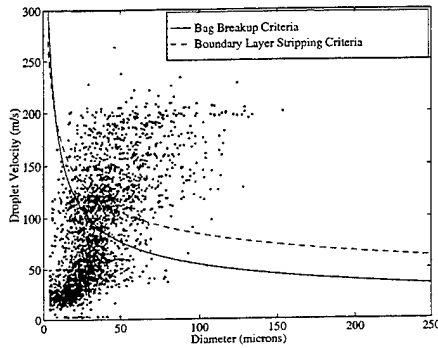

Figure 30. Comparison of 105 MPa injection pressure droplet data
at z = 6 cm, r = 0 mm with droplet breakup criteria.
The surrounding gas velocity is assumed to be zero.

In comparison with Figure 27, Figure 31 shows the low pressure diesel spray data for the same location. The surrounding gas velocity is assumed to be equivalent to the average droplet velocity at that time. There are a couple differences. First, there are still many droplets larger than 150 μm at this distance unlike in the high pressure case where such large droplets disappeared. In addition, the high pressure case had several data points exceeding the bag breakup and BLS breakup criteria. The low pressure case does indicate that some droplets would be subject to bag breakup, but there is only one point exceeding the BLS criteria.
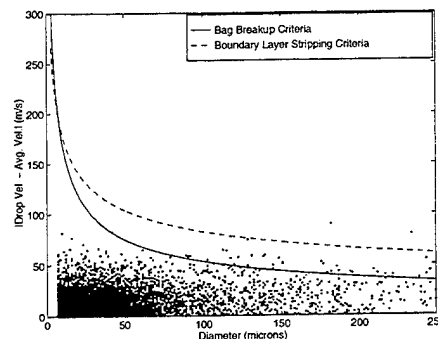

Figure 31. Comparison of 21 MPa injection pressure droplet data
at z = 6 cm, r = 0 mm with droplet breakup criteria. The
droplet relative velocity is assumed to be the absolute

value of the droplet velocity minus the average droplet
velocity at that time in the spray.

Figure 32. Comparison of 21 MPa injection pressure droplet data
at z = 3 cm, r = 0 mm with droplet breakup criteria. The
droplet relative velocity is assumed to be the absolute
value of the droplet velocity minus the average droplet
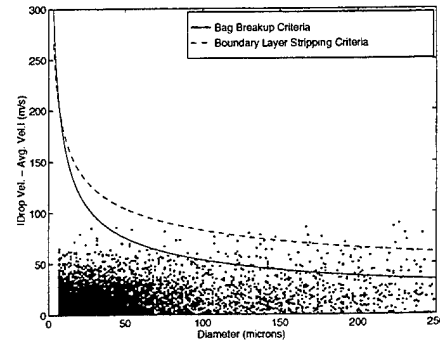velocity at that time in the spray.

Traveling back towards the nozzle, there is not much variation in the low pressure case on-axis data with respect to the breakup criteria. Figure 32 shows the phase/Doppler data for the on-axis case of x = 3 cm. While the data in this figure indicates slightly higher velocities and more numerous large droplets, there is little variation from Figure 31 despite 3 cm of travel. This is opposite of the trend seen in the high injection pressure data, confirming that injection pressure has a significant effect upon the spray droplet distribution.

Off-axis data is shown in Figure 33 for the high pressure spray along with breakup criteria boundaries. The droplet data was taken at the location z = 3 cm, r = 3 mm. The surrounding gas velocity is assumed to be zero, although in reality the spray would have imparted some velocity to the gas despite the off-axis position. The plot shows that almost all of the droplets are stable. Only a few points surpass the bag breakup criteria and fewer still surpass the BLS criteria.
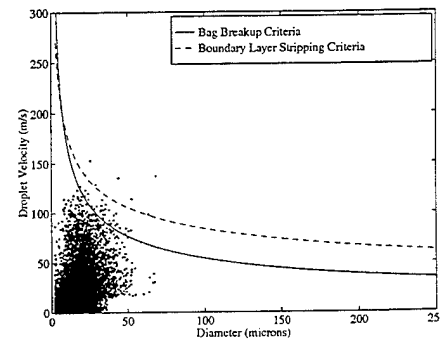

Figure 33. Comparison of 105 MPa injection pressure droplet data
at z =3 cm, r = 3 mm with droplet breakup criteria. The
surrounding gas velocity is assumed to be zero.

Figure 34 presents the low pressure Diesel spray case of Figure 33. The low pressure case only has a few droplets in excess of the bag breakup criteria and none beyond the BLS criteria. The rest of the

droplets are stable as in the high pressure case. The plot also shows that the droplets appear to fall into two groupings. Some of the droplets have no variation in velocity with size while the primarily smaller droplets exhibit a proportional velocity-size correlation. In the high pressure case, there does not appear to be any such correlation unless it is one with a very steep slope.
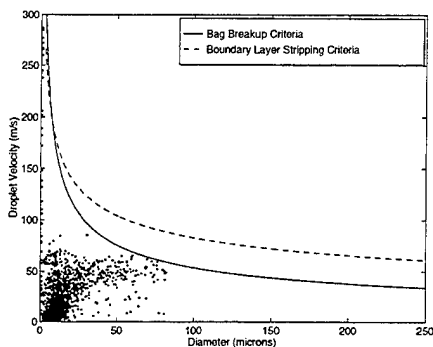

Figure 34. Comparison of 21 MPa injection pressure droplet data at z = 3 cm, r = 3 mm with droplet breakup criteria. The surrounding gas velocity is assumed to be zero.

Figure 35. Comparison of 105 MPa injection pressure droplet data at z = 6 cm, r = 5 mm with droplet breakup criteria. The surrounding gas velocity is assumed to be zero.

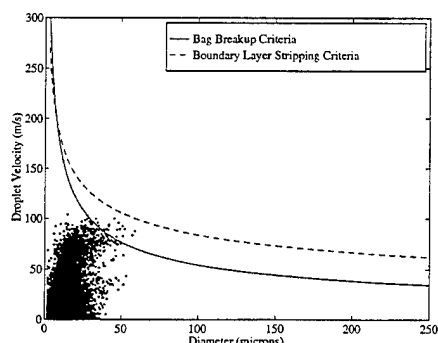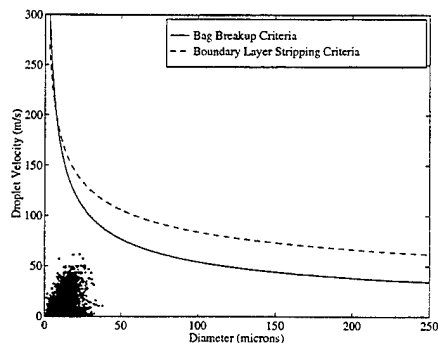*Figure 36. Comparison of 105 MPa injection pressure droplet data at z = 6 cm, r = 9 mm with droplet breakup criteria. The surrounding gas velocity is assumed to be zero.*

Figure 35 and Figure 36 display the droplet data for off-axis locations z = 6 cm, r = 5 mm and z = 6 cm, r = 9 mm, respectively, for the high pressure diesel spray and how they lie with respect to the breakup criteria. In Figure 35, no droplets would be subject to boundary layer stripping and only a few would face bag breakup. For the z = 6 cm, r = 9 mm location, the fringe of the spray, all the droplets are stable. The droplet data in either figure does not present any visible velocity-diameter correlation.

CONCLUSION

The use of high injection pressure spray system appears to have several notable effects upon Diesel spray droplets. In addition to increasing the overall droplet velocities, it changes the tip of the velocity profile near the nozzle to the region with the fastest droplets. Eventually, the velocity profile reverts to a profile similar to that of a low injection pressure system with the fastest droplets in the middle of the spray.

Increased injection pressure also appears to increase the droplet number density in the head of the spray, making examination difficult. These regions of high number density initially grow with distance from the nozzle. At the same time, drop sizes decrease rapidly from the initial broad diameter distribution.

In comparison, a low injection pressure spray system tended to maintain the large droplets found in the initial distribution near the nozzle. Regions of high number densities still existed for the low injection pressure spray system but not nearly to the extent of the high pressure system.

The high injection pressure system also made the spray droplets near the nozzle susceptible to breakup processes. However, with rapid declines in droplet diameters, droplets further away from nozzle became less susceptible to aerodynamic breakup even though they still possessed velocities of up to 200 m/s.

13

REFERENCES

1. Pitcher, G. and Wigley, G., "Velocity and Dropsize Measurements in Fuel Sprays in a Direct Injection Diesel Engine," International Conference on Mechanics of Two-Phase Flows, 1989.

2. Coghe, A. and Cossali, G. E., "Characterization of Unsteady Diesel Sprays by Phase Doppler Anemometry," Fourth International Conference on Laser Anemometry, Advances and Applications, Vol. 2, 1991.

3. Pitcher, G. and Wigley, G., "The Droplet Dynamics of Diesel Fuel Sprays Under Ambient and Engine Conditions," Fourth International Conference on Laser Anemometry, Advances and Applications, Vol. 2, 1991.

4. Hardalupas, Y., Taylor, A., and Whitelaw, J., "Characteristics of the Spray from a Diesel Injector", Int. J. Multiphase Flow, Vol. 18, No. 2, pp. 159-179, 1992.

5. Quoc, H. X. and Brun, M., "Study on Atomisation and Fuel Drop Size Distribution in Direct Injection Diesel Spray," SAE Paper 940191, 1994.

6. Payri, F., Desantes, J. M., and Arrègle, J., "Characterization of D.I. Diesel Sprays in High Density Conditions," SAE Paper 960774, 1996.

7. Kato, T., Tsujimura, K., Shintani, M., Minami, T., and Yamaguchi, I., "Spray Characteristics and Combustion Improvement of D.I. Diesel Engine with High Pressure Fuel Injection," SAE Paper 890265, 1989.

8. Minami, T., Yamaguchi, I., Shintani, M, Tsujimura, K., and Suzuki, T., "Analysis of Fuel Spray Characteristics and Combustion Phenomena under High Pressure Fuel Injection," SAE Paper 900438, 1990.

9. Yunyi, G. and Xuanming, L., "The Effect of Ambient Gas Temperature and Density on the Development and Wall Impingement of High-Injection Pressure Diesel Fuel Sprays," Trans. of the ASME, J. of Eng. for Gas Turbines and Power, Vol. 115, No. 4, Oct. 1993, pp. 777-780.

10. Su, T. F. and Farrell, P. V., "Nozzle Effect on High Pressure Diesel Injection," SAE Paper 950083, 1995.

11. Nishida, M, Nakahira, T., Komori, M., Tsujimura, K. and Yamaguchi, I., "Observation of High Pressure Fuel Spray with Laser Light Sheet Method," SAE Paper 920459, 1992.

12. Koo, J. Y., "Characteristics of a Transient Diesel Fuel Spray," Ph.D. thesis, Department of Mechanical Engineering, University of Wisconsin-Madison, 1991.

13. Koo, J. Y. and Martin, J. K., "Droplet Sizes and Velocities in a Transient Diesel Fuel Spray," SAE Paper 900397, 1990.

14. Koo, J. Y. and Martin, J. K., "Near-Nozzle Characteristics of a Transient Fuel Spray," Atomization and Sprays, Vol. 5, pp. 107-121, 1995.

15. Reitz, R.D. and Diwakar, R., "Effect of Drop Breakup on Fuel Sprays," SAE Paper 860469, 1986.